Perspectives on scaling and multiscaling in passive scalar turbulence

Tirthankar Banerjee[*] and Abhik Basu[†]
Condensed Matter Physics Division, Saha Institute of Nuclear Physics, Calcutta 700064, India

(Received 14 February 2018; revised manuscript received 24 April 2018; published 17 May 2018)

We revisit the well-known problem of multiscaling in substances passively advected by homogeneous and isotropic turbulent flows or *passive scalar turbulence*. To that end we propose a two-parameter continuum hydrodynamic model for an advected substance concentration θ, parametrized jointly by y and $\overline{y}$, that characterize the spatial scaling behavior of the variances of the advecting stochastic velocity and the stochastic additive driving force, respectively. We analyze it within a one-loop dynamic renormalization group method to calculate the multiscaling exponents of the equal-time structure functions of θ. We show how the interplay between the advective velocity and the additive force may lead to simple scaling or multiscaling. In one limit, our results reduce to the well-known results from the *Kraichnan model* for passive scalar. Our framework of analysis should be of help for analytical approaches for the still intractable problem of fluid turbulence itself.

DOI: 10.1103/PhysRevE.97.052124

I. INTRODUCTION

The advection of a passive substance, e.g., a colorant dye in water, moisture mixing in air, or a weakly heated flow, such as an air jet (i.e., advection of temperature), by turbulent flows, more known as *passive scalar turbulence*, stands as a good example of driven nonequilibrium systems; see Ref. [1] for detailed discussions on this topic. The concentration of such an advected substance can exhibit complex scaling behavior in the nonequilibrium steady state (NESS) that shows remarkable phenomenological parallels with the behavior in fully developed hydrodynamic turbulence, with energy pumping at large scales (integral scale) L and viscous dissipation occurring mainly at small viscous scales η_d [2]. The NESS in homogeneous and isotropic fluid turbulence is characterized by the *multiscaling* of equal-time structure functions $\mathcal{S}_n^v(r)$ of the longitudinal component of the velocity increments $\Delta v(r) = \hat{\mathbf{r}} \cdot [\mathbf{v}(\mathbf{x}+\mathbf{r},t) - \mathbf{v}(\mathbf{x},t)]$, $\hat{\mathbf{r}}$ being the unit vector along $\mathbf{r}$ (separation vector between two points): $\mathcal{S}_n^v(r)$ is defined as

$$\mathcal{S}_n^v(r) = \langle |\Delta v(\mathbf{r})|^n \rangle. \tag{1}$$

It was originally argued [3] that $\mathcal{S}_n^v(r)$ in homogeneous and isotropic fully developed turbulence are independent of both L and η_d in the inertial regime $L \gg r \gg \eta_d$ and display *universal scaling*, $\mathcal{S}_n^v(r) \sim r^{\zeta_n^v}$, $\zeta_n^v = n/3$, a linear dependence on n corresponding to simple scaling. Subsequent detailed studies, both experimental and numerical, revealed corrections to these scaling making ζ_n^v depend nonlinearly upon n in a way not known in a closed form, a feature known as *multiscaling* [2,4]; debate still persists on whether these corrections depend on L or η_d or both. In particular, $\zeta_n^v < n/3$ for $n < 3$, where as $\zeta_n^v > n/3$ for all $n > 3$ are found; $\zeta_3 = 1$ is one of the few exact results of fluid turbulence, known as the *von Kármán–Howarth 4/5th* law [2]. Despite the mounting experimental and numerical results, a self-consistent microscopic theory for multiscaling starting from the forced Navier-Stokes equation still remains elusive. In fact, renormalization group approaches that have been immensely successful in studies on universal critical phenomena and critical dynamics [5] have not met with similar success in understanding of the universal multiscaling in fully developed fluid turbulence; see Ref. [6] for detailed discussions on renormalization group approaches to fluid turbulence.

Difficulties in theoretical studies of fluid turbulence prompted scientists to search for simpler models that would show similar scaling behavior and at the same time would allow for controlled analytical approaches. The investigation of the statistics of the passive scalar field advected by random flows offers great insight into the origin of intermittency and multiscaling observed in fluid turbulence. A passive scalar has no dynamical effects (e.g., buoyancy) on the advecting fluid motion itself; i.e., the fluid motion remains autonomous, independent of the embedded concentrations. In the well-known *Kraichnan model* for passive scalar turbulence [7,8], the incompressible velocity field is *given* and assumed to obey a zero-mean Gaussian distribution with a variance that is spatially long range but temporally δ-correlated as opposed to being obtained from the solutions of the forced Navier-Stokes equation. This reduces the problem to a theory linear in the concentration θ for a given Gaussian-distributed velocity, making the problem analytically amenable. This model has been extensively studied by a variety of analytical means, ranging from field-theoretic perturbation theories [9] to zero-mode analyses [10] and nonperturbative methods [11] among others, which yield for the scaling of the equal-time, even order structure concentration functions

$$\mathcal{S}_{2n}(r) \equiv \langle [\theta(\mathbf{x}+\mathbf{r}) - \theta(\mathbf{x})]^{2n} \rangle \sim r^{\zeta_{2n}}, \tag{2}$$

where we have suppressed the time labels of θ; $r = |\mathbf{r}|$ in the inertial range. The scaling exponents ζ_{2n} turn out to be nonlinear functions of order n, reminiscent of multiscaling in fluid turbulence (see below). The odd order structure

[*]tirthankar.banerjee@saha.ac.in
[†]abhik.basu@saha.ac.in; abhik.123@gmail.com

functions vanish identically due to the linear dependence of the Kraichnan model on θ (see below). In this model, as described below, the external (additive) stochastic force is assumed to have a nonvanishing variance concentrated only at the largest scales. The zero-mean, Gaussian-distributed velocity field $\mathbf{v}(\mathbf{r},t)$, assumed incompressible, has a variance

$$\langle v_i(\mathbf{q},t)v_j(-\mathbf{q},0)\rangle = \frac{\tilde{D}P_{ij}(\mathbf{q})\delta(t)}{(q^2+1/L^2)^{\epsilon}} \tag{3}$$

in the Fourier space in the Kraichnan model [9,10]; see also Ref. [12]. Here, v_i is the ith component of $\mathbf{v}$, i,j are the Cartesian indices; $\tilde{D}$ is a constant, $\mathbf{q}$ is a Fourier wave vector, and $P_{ij} = \delta_{ij} - q_iq_j/q^2$ is the transverse projection operator; L is a large length scale of about system size. In the lowest-order perturbation theory, the multiscaling exponents have been found to be

$$\zeta_{2n} = 2n - \frac{n\epsilon(d+2n)}{d+2}, \tag{4}$$

with ϵ as the expansion parameter, d as the space dimension. This has been studied numerically as well; see, e.g., Refs. [13,14]. Passive scalar turbulence has also been studied in turbulent atmospheric convection [15] and in low-temperature helium flows [16]. The scaling laws of a passive scalar in fully developed turbulence have been studied experimentally [17]. The Kraichnan passive scalar model has been subsequently extended to include various different effects, e.g., compressibility of the fluid [18], effects of a mean gradient [19], effects of shear flows [20], and random shear flows [21].

In the present work, we revisit the problem of scaling and multiscaling in a passively advected substance concentration θ. To that end, we construct hydrodynamic models for θ, akin to the well-known *Kraichnan model* for passive scalar advection [7,8], driven by a stochastic advecting velocity $\mathbf{v}$ and an additive force f. The dynamics of θ is controlled jointly by y and $\overline{y}$, spatial scaling exponents of the variances respectively of $\mathbf{v}$ and f. By using Wilson momentum shell dynamic renormalization group (DRG) and within a one-loop perturbation approximation, we elucidate scaling and multiscaling in these models. In particular, we calculate the multiscaling exponents ζ_{2n} that depend linearly (in the case of simple scaling) or nonlinearly (in the case of multiscaling) on n and are parametrized by y and $\overline{y}$. We also show that in the inertial range, $\mathcal{S}_{2n}(r)$ explicitly depends on L which ultimately leads to multiscaling (or lack thereof). We establish the crucial role played by *both* the advecting velocity and the additive noise in the dynamical equation for θ. We, in particular, show how the spatial scaling of the variance of the additive stochastic force affects ζ_{2n}. Our calculational framework directly extends the standard DRG calculations for scaling in driven diffusive models [22].

The rest of this article is organized as follows: In Sec. II, we introduce the two models, model I and model II, for advected passive scalar turbulence that differ in the variance of the Gaussian distributed $\mathbf{v}$. In Sec. III, we analyze the scaling in the linear model. Then in Sec. IV, we show the renormalization group analysis for the relevant model parameters. Next, in Secs. V and VI we calculate the scaling and multiscaling exponents in model I and model II, respectively. We demonstrate that multiscaling ensues only when both the advective velocity and additive forcing have long-range spatial correlations. In Sec. VII we summarize and conclude. We provide some technical details in appendices for the interested reader.

II. MODELS FOR PASSIVELY ADVECTED SCALARS

Let substance concentration field $\theta(\mathbf{x},t)$ be passively advected by an incompressible velocity field $\mathbf{v}$ and forced by an additive stochastic force f. The equation of motion (EOM) for θ takes the form [7,8]

$$\frac{\partial\theta}{\partial t} + \lambda\mathbf{v}\cdot\boldsymbol{\nabla}\theta = \nu\nabla^2\theta + f, \tag{5}$$

where $\mathbf{v}$ is a fluctuating velocity field, λ a nonlinear coupling constant, ν the diffusivity. We ignore any mean concentration gradient across the system, i.e., $\langle\boldsymbol{\nabla}\theta\rangle = 0$. Stochastic function f is a zero-mean Gaussian noise with variance in the Fourier space given as

$$\langle f(\mathbf{q},t)f(-\mathbf{q},0)\rangle = 2D_0q^{-\overline{y}}\delta(t). \tag{6}$$

Here for $\overline{y} = -2$, the noise f becomes the standard conserved noise, which we first consider. We then generalize for arbitrary $\overline{y}$. Further, $D_0 > 0$ sets the amplitude of the additive noise f. Also $\mathbf{q}$ is a wave vector and $q = |\mathbf{q}|$.

For realistic, naturally occurring incompressible systems in three dimensions (3D), $\mathbf{v}$ follows the (incompressible) 3D Navier-Stokes equation, which itself displays anomalous scaling or *multiscaling* when forced at large scales. However, traditionally in passive scalar problems $\mathbf{v}$ is assumed to be a given input as a zero-mean Gaussian distributed field with a given variance that is spatially long range. We write $D^v_{ij}(\mathbf{q},\omega)$ as the variance of $\mathbf{v}$ in the Fourier space:

$$\langle v_i(\mathbf{q},\omega)v_j(-\mathbf{q},-\omega)\rangle = D^v_{ij}(\mathbf{q},\omega). \tag{7}$$

Equivalently, in the time domain

$$\langle v_i(\mathbf{q},t)v_j(-\mathbf{q},0)\rangle = D^v_{ij}(\mathbf{q},t). \tag{8}$$

In particular, we assume

$$D^v_{ij}(\mathbf{q},t) = D_1P_{ij}(\mathbf{q})q^{-y}\exp(-\Gamma t); \tag{9}$$

$D_1 > 0$ is a constant that sets the amplitude of the variance D^v_{ij}, and the exponent $y > 0$. Parameter $\Gamma > 0$ controls the temporal decay of the time-dependent velocity correlator and parametrizes (9). We consider two specific choices for Γ.

(i) Model I: $\Gamma \to \infty$ with D_1 scaling with Γ, i.e., $D_1/\Gamma = A > 0$ a constant. Relaxation of the velocity modes is independent of wave vector $\mathbf{q}$. In that limit, (9) reduces to being temporally δ-correlated:

$$D^v_{ij}(\mathbf{q},t) = AP_{ij}(\mathbf{q})q^{-y}\delta(t). \tag{10}$$

Such a flow field can arise, e.g., in a frictional flow with a large friction and a large external stirring forcing, such that the two balance and in turn produce a flow field correlated as in (10). The flow is self-similar as is evident from (10), but being Gaussian-distributed it is not *intermittent*, unlike turbulent velocity fields obtained from the forced Navier-Stokes equation [2]. This has been used in the literature already [9,12]. Notice that Eq. (5) in conjunction with variances (6) and (10) is invariant under the *Galilean transformation*:

$\mathbf{x}' = \mathbf{x} + \mathbf{c}t, t' = t, \partial/\partial t' = \partial/\partial t - \lambda \mathbf{c}\cdot\nabla$. Here, $\mathbf{c}$ is the Galilean boost. We elucidate below how scaling and multiscaling are parametrized by $\overline{y}, y$. In particular, we show below that the choice $\overline{y} = d$ together with (10) above reproduce the results on the multiscaling of $\mathcal{S}_{2n}(r)$ from the well-known Kraichnan model for passive scalars [7,8].

(ii) Model II: $\Gamma = \eta q^2$. This is equivalent to $\mathbf{v}$ satisfying the linearized Navier-Stokes equation:

$$\frac{\partial v_i}{\partial t} = -\nabla_i P + \eta\nabla^2 v_i + g_i, \tag{11}$$

with $\langle v_i\rangle = 0$; P is the pressure and η the kinematic viscosity. Also, $\mathbf{v}$ is assumed to be incompressible, i.e., $\nabla\cdot\mathbf{v} = 0$. This may be used to eliminate P from (11), yielding

$$\frac{\partial v_i}{\partial t} = \eta\nabla^2 v_i + P_{ij} g_j. \tag{12}$$

Function g_i is a zero-mean Gaussian distributed stochastic force with a variance

$$\langle g_i(\mathbf{q},t) g_j(-\mathbf{q},0)\rangle = \tilde{D}_1 |q|^{-y}\delta(t)\delta_{ij}, \tag{13}$$

where subscripts i, j refer to Cartesian coordinates; $\tilde{D}_1 > 0$. This yields

$$D^v_{ij}(\mathbf{q},\omega) = \frac{2\tilde{D}_1 |q|^{-y} P_{ij}(\mathbf{q})}{\omega^2 + \eta^2 q^4}. \tag{14}$$

Unlike model I, Eqs. (5) and (12) are *not* invariant under the Galilean transformation defined above. The flow in model II implies a low Reynolds number flow due to a large viscosity that makes that advective nonlinear term unimportant. The inertia term nonetheless remains relevant, due to the large forcing. The flow field, as in model I, is self-similar and not regular or streamlined due to the stochasticity of the applied stirring forces. Similarly to model I, $\mathbf{v}$ in model II is not intermittent. It may be noted that model II is a special case of the studies in Refs. [23,24]. Indeed, for $\overline{y} = d + 2$ it would directly correspond to the studies with *frozen* or *time-independent* velocity in Refs. [23,24].

Like model I, we elucidate below how scaling and multiscaling are parametrized by $\overline{y}, y$ in model II. In particular, we show below that the choice $\overline{y} = d + 2$ sets the threshold for multiscaling. Overall we find that the scaling and multiscaling properties of model II are qualitatively similar but quantitatively different from model I.

Variance (9) implies that in the Fourier space

$$D^v_{ij}(q,\omega) = \langle v_i(\mathbf{q},\omega) v_j(-\mathbf{q},-\omega)\rangle = \frac{2D_1 P_{ij}(\mathbf{q}) q^{-y}\Gamma}{\omega^2 + \Gamma^2}, \tag{15}$$

where ω is the Fourier frequency. This yields in the time domain Eq. (10) for $\Gamma \to \infty$ and $D_1/\Gamma = A$, a constant; for model II, we set $\Gamma = \eta q^2$ and $\tilde{D}_1 = D_1\Gamma$. In fact, we note that our correlator given in Eq. (15) with $\Gamma = \eta q^2$ is a specialized case of the velocity correlator given in [23,24], where the velocity fluctuations are assumed to relax with a q-dependent timescale $\sim q^{2-\tilde{\eta}}$. Comparing with [24], we thus find that $\tilde{\eta} = 0$, $u_0 v_0 \to \Gamma$, $D_0/u_0 \sim D_1\Gamma$, and $d - 2 + 2\epsilon = y$ give the necessary correspondence.

III. SCALING IN THE LINEAR MODEL

It is instructive to first analyze the scaling of $\mathcal{S}_{2n}(r)$ without advection, i.e., in the linear limit with $\lambda = 0$, for which model I and model II become identical. The flow field decouples from the concentration dynamics, and the latter dynamics can be solved exactly. We illustrate scaling in the linear model for both $\overline{y} > d$ and $\overline{y} < d$. We find

$$\langle|\theta(\mathbf{q},\omega)|^2\rangle = \frac{2D_0 q^{-\overline{y}}}{\omega^2 + \nu^2 q^4}. \tag{16}$$

Equivalently, in the time domain for the equal-time correlator

$$\langle\theta(\mathbf{q},t)\theta(-\mathbf{q},0)\rangle = D_0 \exp(-\nu q^2|t|)\frac{1}{q^{2+\overline{y}}}. \tag{17}$$

This then allows us to obtain the scaling of the equal-time second-order structure function

$$\mathcal{S}_2(r) = 2\langle\theta(\mathbf{x},t)^2\rangle - 2\langle\theta(\mathbf{x},t)\theta(0,t)\rangle, \tag{18}$$

which may be obtained from (17) by inverse Fourier transform:

$$\mathcal{S}_2(r) = \int_{2\pi/L}^{\Lambda} \frac{d^d q}{(2\pi)^d} D_0 \frac{1}{q^{2+\overline{y}}}[1 - \exp(i\mathbf{q}\cdot r)], \tag{19}$$

where L is the linear system size and Λ is an upper cutoff; Λ corresponds to a microscopic length scale $2\pi/\Lambda$ at which the continuum descriptions break down.

For $\overline{y} < d$, (19) is insensitive to the lower limit, which can be brought to zero (i.e., $L \to \infty$) without encountering any divergence. We find

$$\mathcal{S}_2(r) \sim r^{2-d+\overline{y}}. \tag{20}$$

Thus, $\mathcal{S}_2(r)$ remains finite as $L \to \infty$ for $\overline{y} < d$. Higher-order structure functions $\mathcal{S}_{2n}(r)$, $n > 1$, can be found easily by noting that in the linear model $\theta(\mathbf{x},t)$ is Gaussian-distributed. This immediately yields

$$\mathcal{S}_{2n}(r) \sim r^{n(2-d+\overline{y})} \tag{21}$$

that, as expected, remains finite for $L \to \infty$. We then find $\zeta_{2n} = n(2 - d + \overline{y})$, rising linearly with $\overline{y}$.

In contrast for $\overline{y} > d$, (19) is dominated by the lower limit yielding

$$\mathcal{S}_2(r) \sim \int \frac{d^d q}{(2\pi)^d} D_0 \frac{(\mathbf{q}\cdot\mathbf{r})^2}{q^{2+\overline{y}}} \sim r^2 L^{\overline{y}-d} \tag{22}$$

in the asymptotic limit $L \gg r$ (corresponding to the inertial range). Clearly, $\mathcal{S}_2(r)$ diverges as $L \to \infty$. This divergence is intimately connected to the divergence of the variance of the noise $f(\mathbf{x},t)$ in (5), when expressed in the real space, for $\overline{y} > d$. Variation of ζ_2 with $\overline{y}$ is shown schematically in Fig. 1.

Similar arguments to those above apply equally well for higher-order structure ($n > 1$). For instance, for $n = 2$

$$\begin{aligned}\mathcal{S}_4(r) &= \langle[\theta(\mathbf{x}+\mathbf{r}) - \theta(\mathbf{x})]^4\rangle \\ &\sim \langle[\theta(\mathbf{x}+\mathbf{r}) - \theta(\mathbf{x})]^2\rangle^2 \sim \mathcal{S}_2(r)^2\end{aligned} \tag{23}$$

using the fact that in the linear theory $\theta(\mathbf{x})$ is Gaussian distributed. Now using $\mathcal{S}_2(r) \sim r^2 L^{\overline{y}-d}$ as obtained above, we

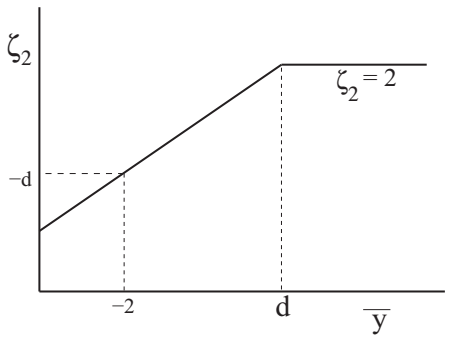

FIG. 1. Schematic plot of ζ_2 versus $\overline{y}$ for the linearized theory. Clearly, ζ_2 is independent of $\overline{y}$ for $\overline{y} \geqslant d$. Here, ζ_2 is continuous everywhere.

find

$$\mathcal{S}_4(r) \sim r^4 L^{2\overline{y}-2d}. \tag{24}$$

In general, it may be established in a straightforward way that

$$\mathcal{S}_{2n}(r) \sim r^{2n} L^{n(\overline{y}-d)}, \tag{25}$$

giving $\zeta_{2n} = 2n$, which is independent of $\overline{y} > d$. Evidently, $\mathcal{S}_{2n}(r)$ diverges for $L \to \infty$. The linear dynamical equation for θ ensures that $\zeta_{2n} \propto n$, implying simple scaling for all values of $\overline{y}$. We show below that in the nonlinear problems ($\lambda \neq 0$) with $y \to d_+$, one still obtains simple scaling for $\overline{y} < d$ with $\mathcal{S}_{2n}(r)$ remaining finite for $L \to \infty$, whereas for $\overline{y} > d$, ζ_{2n} becomes a nonlinear function of n; i.e., multiscaling ensues with $\mathcal{S}_{2n}(r)$ diverging for $L \to \infty$. The values of the scaling exponents depend on the model, i.e., model I or model II. We set out to analyze the nonlinear cases below.

IV. RENORMALIZATION GROUP ANALYSIS

We begin by writing down the dynamic action functional $S_{\rm act}$ for the system [25], averaged over the noise f:

$$S_{\rm act} = \int d^d q\, d\omega \Big\{ D_0 q^2 \hat{\theta}(\mathbf{q},\omega)\hat{\theta}(-\mathbf{q},-\omega) + \hat{\theta}(-\mathbf{q},-\omega)\Big[-i\omega\theta(\mathbf{q},\omega) + i\lambda q_m \sum_{\mathbf{q}_1,\Omega} v_m(\mathbf{q}_1,\Omega)\theta(\mathbf{q}-\mathbf{q}_1,\omega-\Omega) + \nu q^2\theta(\mathbf{q},\omega)\Big]$$
$$- v_i(\mathbf{q},\omega)\big[D^v_{ij}(q,\omega)\big]^{-1} v_j(-\mathbf{q},-\omega)/2\Big\}, \tag{26}$$

where $\hat{\theta}$ is the usual response field [25] and Ω is a frequency. We now set out to calculate the scaling of $\mathcal{S}_{2n}(r)$, the structure functions of θ. As a first step, we perturbatively calculate fluctuation corrections to the model parameters ν, D_0, and λ in (26) up to the one-loop order. Due to the long-range nature of (10) and the conservation law form of the dynamics of θ, these one-loop corrections diverge in the infrared limit, and as a result, naive perturbation theory breaks down. In order to deal with these long-wavelength divergences in a systematic manner, we employ Wilson momentum shell dynamic renormalization group (DRG) [26–28]; see also Ref. [29] for detailed discussions on DRG applications to dynamic critical phenomena. To this end, we first integrate out fields $\theta(\mathbf{q},\omega), \hat{\theta}(\mathbf{q},\omega), v_i(\mathbf{q},\omega)$ with wave vector $\Lambda/b < q < \Lambda$, $b > 1$ is dimensionless, perturbatively up to the one-loop order in (26). Here, Λ is an upper cutoff for the wave vector. This allows us to obtain the "new" model parameters $\nu^<, D_0^<$, and $\lambda^<$ corresponding to a modified action $S^<_{\rm act}$ with an upper cutoff $\Lambda/b < \Lambda$. We first consider $\overline{y} = -2$ corresponding to conserved additive noises, and subsequently study $\overline{y} > -2$. We obtain

$$\nu^< = \nu + \frac{K_d(d-1)D_1\lambda^2}{d}\int_{\Lambda/b}^{\Lambda} dq\, \frac{q^{d-1-y}}{\Gamma+\nu q^2}, \tag{27}$$

where K_d is a solid angle factor coming from the d-dimensional integral, and Λ is an upper wave vector cutoff. Now for $\overline{y} = -2$ there are diverging corrections to D_0 yielding

$$D_0^< = D_0 + \frac{\lambda^2 D_1 D_0 K_d(d-1)}{\nu d}\int_{\Lambda/b}^{\Lambda} dq\, \frac{q^{d-1-y}}{\Gamma+\nu q^2}. \tag{28}$$

On the other hand, for $\overline{y} > -2$, there are no relevant fluctuation corrections to D_0. This may be understood as follows. It is evident from the action functional (26) or the equation of motion (5) together with the incompressibility of the velocity field that each vertex is $O(q)$, yielding any putative one-loop correction to the variance (6) at $O(q^2)$. For $\overline{y} = -2$, this evidently yields a relevant correction in a perturbation theory. On the other hand, for $\overline{y} > -2$, the bare noise variance is $O(q^{-\overline{y}})$, making the one-loop perturbative corrections less relevant in the long-wavelength limit than the corresponding bare contribution. This explains the lack of any relevant fluctuation corrections to D_0 for $\overline{y} > -2$. We further note that there is no relevant (in a DRG sense) correction to λ for both model I and model II. For model I, this is a consequence of the Galilean invariance. For model II, there is no Galilean invariance; however, the most relevant correction appears at $O(q^2)$, while the vertex is $O(q)$. This renders the fluctuation corrections to λ *irrelevant* in a scaling sense in model II. Thus

$$\lambda^< = \lambda. \tag{29}$$

See Appendix B for the relevant one-loop Feynman diagrams.

V. MULTISCALING IN MODEL I

To study multiscaling in model I, we set $\Gamma \to \infty$ with $\frac{D_1}{\Gamma} = A$, a finite constant. The values of the different one-loop contributions listed above are evaluated in Appendix B. Next we rescale space in the form $\mathbf{x} \to \mathbf{x}' = \mathbf{x}/b$ and time according to $t \to t' = t/b^z$, z being the dynamic exponent. The corresponding wave vector and frequency respectively scale as $q' = bq$ and $\omega' = b^z\omega$. Under this rescaling scheme, let θ scale according to $\theta(\mathbf{x},t) = \theta(b\mathbf{x}', b^z t') = \xi_R\theta(\mathbf{x}',t') = b^\chi\theta(\mathbf{x}',t')$ with $\xi_R = b^\chi$ and $\mathbf{v}(\mathbf{x},t) = \xi_{vR}\mathbf{v}(\mathbf{x}',t')$. Here, χ is

the spatial scaling exponent of θ. In the linear limit, these exponents can be read off exactly for the correlation function:

$$z = 2,\ \chi = (z - d + \overline{y})/2 = (2 - d + \overline{y})/2, \tag{30}$$

which hold for all $\overline{y}$.

Now, exploiting the overall arbitrariness in choosing the rescaling factor, we assume A does not scale and thus get $\xi_{vR} = b^{(y-d-z)/2}$. With $b = \exp[\delta l] \approx 1 + \delta l$ for small δl, we can write down the following continuum recursion relations for the model parameters:

$$\frac{d\nu}{dl} = \nu[z - 2 + g], \tag{31}$$

$$\frac{dD_0}{dl} = D_0[z - 2\chi - d - 2 + g], \tag{32}$$

and

$$\frac{d\lambda}{dl} = \lambda\left[\frac{y + z - d}{2} - 1\right]. \tag{33}$$

Here $g = \frac{\lambda^2 A(d-1)K_d \Lambda^{d-y}}{\nu d}$ is an effective coupling constant. The flow equation for g reads

$$\frac{dg}{dl} = g[y - d - g]. \tag{34}$$

At the DRG fixed point (FP), $dg/dl = 0$. This gives $g^* = 0$, $y - d$ as the FP values for g. Clearly, $g^* = 0$ is the stable FP (trivial FP at which the nonlinear coupling vanishes) for $y \leqslant d$ while $g^* = y - d$ becomes the stable FP for $y > d$ (nontrivial FP at which the nonlinear coupling remains relevant). For the validity of our low-order perturbation theory, we must have $g^* = y - d \ll 1$. We are now in a position to calculate the dynamic exponent z and the spatial scaling exponent χ, as defined earlier.

At the DRG FP, Eq. (31) yields $z = 2 - g$. Hence, for $y \leqslant d$, we have $z = 2$ and for $y > d$, $z = 2 - y + d < 2$. Further, Eq. (32) at the DRG FP gives the value of the exponent $\chi = \frac{z-d-2+g}{2} = -\frac{d}{2}$. For $0 < y < d$, $g = 0$ at the DRG FP, and hence $z = 2$ and $\chi = -d/2$; i.e., nonlinear effects are irrelevant in the long-wavelength limit if $y < d$. Interestingly, χ remains independent of y and is determined only by d, unlike z.

In the linearized limit of model I, scaling exponent χ grows with a rising $\overline{y}$; see Eq. (30). In a low-order perturbative approach, expecting a similar monotonic trend even for the nonlinear problem, we see that multiscaling clearly necessitates the additive noise f in (5) to be sufficiently *long range*, i.e., a larger $\overline{y}$: to study that we set $\overline{y} > -2$. As explained above, with $\overline{y} > -2$ there will now be no relevant corrections to D_0. Proceeding as above, we get

$$\frac{dD_0}{dl} = D_0[z - 2\chi - d + \overline{y}]. \tag{35}$$

Thus at the DRG FP, we have $\chi = \frac{z-d+\overline{y}}{2}$. Again, for $y > d$, we have

$$z = 2 - y + d. \tag{36}$$

Using these relations, we evaluate χ at the FP as a function of y and $\overline{y}$:

$$\chi = \frac{2 - y + \overline{y}}{2}, \tag{37}$$

for all $\overline{y} > -2$. Hence, χ can even be positive depending on y and $\overline{y}$. It now remains to be seen whether multiscaling follows or not for $\overline{y} > -2$. Nontrivial FP $g^* = y - d$ remains unaffected by $\overline{y}$. We continue to assume $g^* \ll 1$ for the validity of the perturbation theory.

With the knowledge of the renormalized model parameters and the associated scaling exponents, we now focus on the structure function $\mathcal{S}_{2n}(r) = \langle[\theta(\mathbf{x} + \mathbf{r}) - \theta(\mathbf{x})]^{2n}\rangle$. On dimensional ground, we expect

$$\mathcal{S}_{2n}(r) = r^{2n\chi} f_n(r/\tilde{L}), \tag{38}$$

where f_n is a dimensionless scaling function of $r/\tilde{L}$, and $\tilde{L}$ is a length scale. Whether $\tilde{L}$ is a "large scale" like the integral scale L, or a "small scale" like the dissipation scale η_d, remains to be seen. We assume

$$f_n(r/\tilde{L}) \sim \left(\frac{\tilde{L}}{r}\right)^{\Delta_{2n}} \tag{39}$$

in the asymptotic scaling regime. If $\Delta_{2n} = 0$, then the scaling function f_n approaches a constant in the asymptotic limit. Nonzero Δ_{2n} with a nonlinear dependence on n may lead to multiscaling.

A. Operator product expansion

Notice that calculation of the structure function $\mathcal{S}_{2n}(r)$ involves averaging of *spatially nonlocal* quantities with respect to the action functional (26). Now we use the idea of the operator product expansion (OPE) [9,30,31] to write

$$[\theta(\mathbf{x} + \mathbf{r}) - \theta(\mathbf{x})]^{2n} \sim \Sigma_m \mathcal{C}_m(r)\mathcal{O}_m(\mathbf{x}), \tag{40}$$

valid for $r/L \ll 1$ (corresponding to the inertial range) where $\mathcal{O}_m(\mathbf{x})$ are the symmetry-permitted *local* composite operators (which are products of the dynamical fields at the same space-time point; see, e.g., Refs. [5,33]), and $\mathcal{C}_m(r)$ are scalar functions of r that should behave in a power-law fashion in the scaling regime. Notice that (40) holds independently of the details of the specific model and even in the noninteracting limit. Since the left-hand side of Eq. (40) is invariant under $\theta \to \theta +$ constant, the right-hand side of (40) must only involve terms which individually respect the same symmetry. Also, the fact that left-hand side of Eq. (40) is a scalar ensures that the operators $\mathcal{O}_m$ that appear on the right-hand side of (40) must also be scalars [9,31]. The leading order operators (in the hydrodynamic limit) are

$$\mathcal{O}_m(\mathbf{x}) = [\nabla_i \theta \nabla_i \theta]^m, \tag{41}$$

where m is zero or any positive integer [32]. Due to the linearity of the θ dynamics as given by Eq. (5), the right-hand side of Eq. (40) can have a composite operator $\mathcal{O}_m$ with a maximum value of m given by $m_{\max} = n$; see Refs. [9,18,23,33]. The expansion series begins with $m = 0$ or the identity operator that does not scale under rescaling of $\mathbf{x}$. Now, as seen from above, θ scales as $b^{\chi} = b^{-d/2}$. This implies that $\mathcal{O}_m(x)$ should naively scale as $b^{-(d+2)m}$ for any m. Thus as m rises, the operator $\mathcal{O}_m(\mathbf{x})$

becomes less relevant in the long-wavelength limit. This means that $m = 0$ becomes the most dominant contribution to $\mathcal{S}_{2n}(r)$.

B. OPE for the linear problem

The idea of OPE in the problem remains true even in the linear limit, for which the fluctuation corrections to all the parameters immediately disappear, and exponents z and χ are given by (30). We now revisit the exactly known scaling of $\mathcal{S}_{2n}(r)$ in the linear case in the context of the OPE discussed above and examine the consistency of the latter. In particular, we try to obtain (22) by using the prescription of OPE as elucidated above: according to that we should have

$$[\theta(\mathbf{x}+\mathbf{r}) - \theta(\mathbf{x})]^2 \sim \mathcal{C}_0(r)\mathbf{I} + \mathcal{C}_2(r)[\partial_i\theta(\mathbf{x})]^2, \tag{42}$$

where $\mathbf{I}$ is the identity operator. Now in the linear theory for $\overline{y} < d$, or $\chi < 1$, the first term on the right-hand side of (42) dominates. This then yields

$$C_0(r) \sim r^{2\chi}, \tag{43}$$

yielding

$$\mathcal{S}_2(r) \sim r^{2\chi} \sim r^{-(2-d+\overline{y})}. \tag{44}$$

Using the linearity of the θ dynamics then,

$$\mathcal{S}_{2n}(r) \sim r^{2\chi} \sim r^{-n(2-d+\overline{y})}, \tag{45}$$

in agreement with (21).

In contrast, for $\overline{y} > d$ or $\chi > 1$ such that the second term on the right-hand side of (42) dominates,

$$\langle[\partial_i\theta(\mathbf{x})]^2\rangle \sim L^{\overline{y}-d}, \tag{46}$$

an L dependence identical to that in (22), giving $\mathcal{C}_2(r) \sim r^2$. Equation (46) clearly shows that

$$\mathcal{S}_2(r) \sim r^2 L^{\overline{y}-d}, \tag{47}$$

unsurprisingly the same as (22). This may be extended to higher-order structure ($n > 1$) easily. For instance for $n = 2$, the most dominant operator that contributes to $\mathcal{S}_4(r)$ in the scaling limit is $[\partial_i\theta(\mathbf{x})]^4$. It is easy to see $\langle[\partial_i\theta(\mathbf{x})]^4\rangle \sim L^{2(\overline{y}-d)}$, giving $\mathcal{C}_4(r) \sim r^4$. Putting together everything then,

$$\mathcal{S}_4(r) \sim r^4 L^{2\overline{y}-2d}, \tag{48}$$

the same as that obtained by direct calculations above. This lends credence to our analysis even when $\lambda \neq 0$. Having reestablished the exactly known scaling exponents of $\mathcal{S}_{2n}(r)$ in the linear limit by the arguments of OPE, we now analyze the nonlinear cases below.

C. OPE for model I

In order to have a one-loop renormalized theory for multiscaling we must now find out how the naive scaling of $\mathcal{O}_m(\mathbf{x})$ changes due to fluctuations. This will allow us to determine the most dominant term in (40) within a one-loop renormalized theory. To this end, we are now basically left with calculating the one-loop renormalization of $\mathcal{O}_n(\mathbf{x})$ for arbitrary n and then find the scaling forms for the renormalized composite operators; see Appendix C for the relevant one-loop Feynman diagram contributing to the renormalization of $\mathcal{O}_m(\mathbf{x})$. We find

$$\langle\mathcal{O}_m^<(\mathbf{x})\rangle = \langle\mathcal{O}_m(\mathbf{x})\rangle[1 + \delta m'], \tag{49}$$

where

$$\begin{aligned}\delta m' &= \frac{\lambda^2 Am(d-1)(d+2m)}{\nu d(d+2)}\int_{\Lambda/b}^{\Lambda}\frac{d^dq}{(2\pi)^dq^y}\\ &= \frac{\lambda^2 Am(d-1)(d+2m)\Lambda^{d-y}K_d}{\nu d(d+2)}\left[1-\frac{1}{b^{d-y}}\right]\\ &= gm\frac{d+2m}{d+2}\left[1-\frac{1}{b^{d-y}}\right] = \delta m\left[1-\frac{1}{b^{d-y}}\right],\end{aligned} \tag{50}$$

where $\delta m = gm(d+2m)/(d+2)$. Now using the same spatial and temporal rescaling procedure as above, we can write

$$\langle\mathcal{O}_m\rangle' = \mathcal{O}_m[b^{2m(\chi-1)} + \delta m']. \tag{51}$$

This yields

$$\langle\mathcal{O}_m(\mathbf{x})\rangle \sim L^{2m(\chi-1)+\delta m} \sim L^{\Delta_{2m}}, \tag{52}$$

where $\Delta_{2m} = 2m(\chi-1) + \delta m$. It remains to be seen which of $\mathcal{O}_m$ dominates in (40). If $\mathcal{O}_m(\mathbf{x})$ ($m \leqslant n$) is the leading order operator (in a DRG sense) for $m = m_0$, comparing with Eqs. (38) and (39) we can write

$$\mathcal{S}_{2n}(r) \sim r^{2n\chi-\Delta_{2m_0}}L^{\Delta_{2m_0}} \sim r^{\zeta_{2n}}, \tag{53}$$

where $\tilde{L}$ is now identified with L as the length scale in the scaling functions f_n. This is consistent with the dependence of $\mathcal{S}_{2n}(r)$ on L in the linear limit, as illustrated above. Thus the scaling function f_n indeed depends on the large scale L. If the most dominant contribution on the right-hand side of (40) comes from the unit operator $\mathbf{I}$, then $\Delta_{2m_0} = 0$ in (53), leading to $\mathcal{S}_{2n}(r)$ being L-independent in the asymptotic limit. This only leads to simple scaling: $\zeta_{2n} \propto n$. In general, whether or not multiscaling follows depends on the sign of Δ_{2n}, which in turn depends on the sign of χ, since $\delta n > 0$. We set $\Delta_2 = 0$ as the threshold for multiscaling, as this would imply all $\Delta_{2n} > 0$, $n > 1$ automatically. With $\overline{y} = -2$, i.e., $\chi = -d/2$, this yields

$$-d - 2 + g = 0, \tag{54}$$

setting $g = y - d = d + 2$ a rather high value for which our low-order renormalized perturbation theory is not expected to remain valid. Assuming a low enough $y - d \ll 1$ for our perturbation theory to be valid, all of $\Delta_{2m} < 0, m \geqslant 1$. This makes all of $\mathcal{O}_m(\mathbf{x})$, $m \geqslant 1$ irrelevant. Thus in this case the dominant contribution to (40) comes from the identity operator $\mathbf{I}$, which in turn gives

$$\mathcal{S}_{2n}(r) = \mathcal{A}_n r^{2n\chi} = \mathcal{A}_n r^{-nd}, \tag{55}$$

where $\mathcal{A}_n$ is the amplitude that does not depend upon L or η_d. Thus we identify

$$\zeta_{2n} = -nd, \quad \zeta_2 = -d, \tag{56}$$

a linear function of n, corresponding to *simple scaling* [34]. We then conclude that there is no multiscaling in the system. In order to have multiscaling from $\mathcal{O}_m(\mathbf{x})$, the dominant contribution to $\mathcal{S}_{2n}(r)$ must come from $m > 0$. This would require the scaling dimension of $\theta(\mathbf{x})$ to be positive so that $\mathcal{O}_m(\mathbf{x})$ grows under spatial rescaling. In fact, renormalized $\mathcal{O}_m(\mathbf{x})$ with the largest positive scaling dimension will determine the multiscaling exponents ζ_{2n}.

From (37), χ rises monotonically with $\overline{y}$. Thus, for sufficiently large $\overline{y}$, $\Delta_{2m} > 0$ is expected. Assuming positive Δ_{2m}, we note that Δ_{2m} becomes maximum for $m = n$; i.e., Δ_{2n} provides the most *dominant* contribution in (40). In that case, with $\tilde{L} = L$ as before, the r dependence of $\mathcal{S}_{2n}(r)$ is thus given by

$$r^{2n\chi-2n(\chi-1)-\delta n} \sim r^{2n-\delta n} \sim r^{\zeta_{2n}}. \tag{57}$$

Here

$$\zeta_{2n} = 2n - \frac{ng(d+2n)}{d+2}. \tag{58}$$

Now for $y > d$, we have at FP, $g = g^* = y - d$. Therefore the structure functions $\mathcal{S}_{2n}(r)$ at FP scale with an exponent,

$$\zeta_{2n} = 2n - \frac{n(y-d)(d+2n)}{d+2}, \tag{59}$$

a nonlinear function of n, as expected for multiscaling. Notice that ζ_{2n} in (59) has *no* explicit dependence on $\overline{y}$. However, $\overline{y}$ must be large enough to make (59) valid. In particular for $n = 1$,

$$\zeta_2 = 2 - (y - d) = 2 - \delta_1. \tag{60}$$

Notice that for a fixed $0 < g^* = \delta_1 > 0$, ζ_2 has *no* d dependencies, whereas $\zeta_{2n}, n > 1$, for the higher-order structure functions depends on d explicitly for a fixed g^*. Thus at $d = 3$, $\zeta_2 = 2 - \delta_1$ and $\zeta_{2n} = 2n - n\delta_1(3 + 2n)/5, n > 1$. While the nonlinear dependencies of ζ_{2n} on n do point to multiscaling, the numerical values of ζ_{2n} are parametrized by $\delta_1 > 0$, which cannot be precisely obtained in our theory.

The threshold on $\overline{y}$ for multiscaling can be inferred from Δ_{2n}, which depends on $\overline{y}$ explicitly. We have

$$\Delta_{2n} = 2n(\chi - 1) + \delta n = n(\overline{y} - y) + \frac{(y-d)n(d+2n)}{d+2}. \tag{61}$$

We note that for $n = 1$ and in the limit $\overline{y} = d$, we get $\Delta_2 = 0$. This sets the threshold for multiscaling with all other $\Delta_{2n} > 0$, $n > 1$, for $g^* \ll 1$, which is required for the validity of our perturbation theory. This is the limit where our predictions from model I coincide with those from the usual passive scalar model studies. Unsurprisingly, in Eq. (59) or (61) $g^* = y - d$ plays the role of ϵ in Ref. [9]. Lastly, at the threshold of multiscaling ($\overline{y} = d$), we have $\chi = 1 - (y - d)/2$, which is very close to 1 for $y - d \ll 1$. Thus the threshold for multiscaling in the linear model shifts only marginally in model I. In addition, as $\overline{y}$ rises above d, ζ_{2n} remains unchanged. Therefore, the multiscaling of $\mathcal{S}_{2n}(r)$ remains unaffected by $\overline{y}$, so long as $\overline{y} \geqslant d$. This *freezing* of the multiscaling exponents ζ_{2n} as functions of $\overline{y}$ is analogous to the arguments for freezing of the multiscaling exponents at their "large-scale" values in genuine hydrodynamic turbulence; see Ref. [33] for detailed technical discussions. Thus, the results here provide new impetus to the possibility of modeling large-scale stirring forces in real hydrodynamic turbulence by Gaussian stochastic ones with variances having power-law spatial dependencies as used here. However, $\overline{y}$ affects the L dependence of $\mathcal{S}_{2n}(r)$, controlled by Δ_{2n}; this gets stronger as $\overline{y}$ rises beyond $\overline{y} = d$.

It remains to be seen what happens for $-2 < \overline{y} < d$. Clearly, there is no multiscaling for $\overline{y} < d$, implying only simple scaling is displayed. At the same time, χ now depends on $\overline{y}$ and y; see Eq. (37). Following the logic outlined above, we find

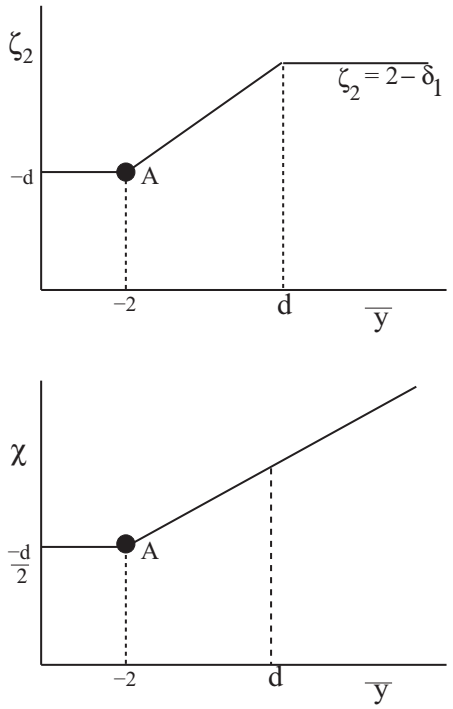

FIG. 2. Schematic plot of ζ_2 (top) and χ (bottom) versus $\overline{y}$ for model I. While both ζ_2 and χ vary linearly with $\overline{y}$ for $-2 < \overline{y} < d$ and have a discontinuity (marked by A) of $O(\delta_1)$ at $\overline{y} = -2$ (where $\delta_1 = y - d > 0$), their respective behaviors are clearly different in the regime of multiscaling, i.e., for $\overline{y} > d$; see text.

$$\zeta_{2n} = 2n\chi = n(2 - y + \overline{y}), \tag{62}$$

$$\zeta_2 = 2\chi = 2 - y + \overline{y}, \tag{63}$$

which rise with $\overline{y}$, as expected. Clearly, (63) smoothly joins (60) at $\overline{y} = d$ as $y \to d$ from above and below. Similarly, (63) yields $\zeta_2 = -d + \mathcal{O}(\delta_1)$ as $\overline{y}$ approaches -2 from above with $y \to d$ from above, which agrees with (56). Thus the discontinuity is $\mathcal{O}(\delta_1)$ as $\overline{y} \to -2$. Thus ζ_2 varies continuously with $\overline{y}$, a conclusion that can be argued to hold for all ζ_{2n}. Schematic plot of χ and ζ_2 versus $\overline{y}$ in model I is shown in Fig. 2.

We thus establish that for the advected substance to display multiscaling, not only should the Gaussian-distributed velocity field have a variance with long-range spatial scaling but the additive noise that drives the dynamics of θ must also have a variance that is spatially long range. We have argued above that $\Delta_2 = 0$ should be the threshold for multiscaling that yields $\overline{y} \geqslant d$ as the necessary condition for multiscaling. At the same time, we must have $y > d$ at the nontrivial fixed point, else the coupling constant vanishes at the DRG FP, rendering the theory effectively *free* with only simply scaling. For $\overline{y} < -2$, a naive perturbation theory generates noise variance that scales as q^2, corresponding to $\overline{y} = -2$. Then all the results obtained for $\overline{y} = -2$ apply for $\overline{y} < -2$ as well. Thus in the y-$\overline{y}$ plane, multiscaling is to be observed only in the region $\overline{y} \geqslant d$ and $y > d$. For $-2 < \overline{y} < d$ and $y > d$, simple scaling given by $\zeta_{2n} = 2n\chi$ with χ as given in (37) together with $z = 2 - y +$

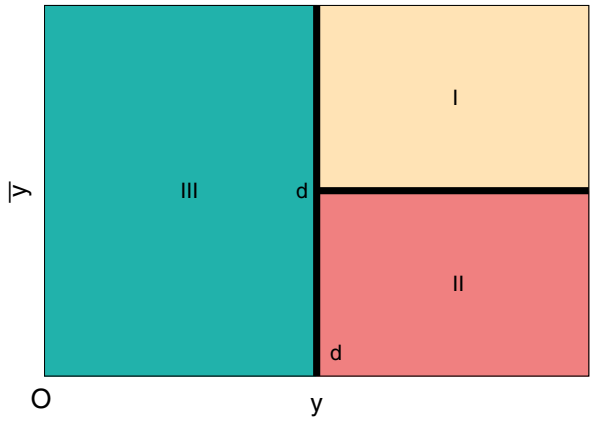

FIG. 3. Phase diagram of model I in the y-$\overline{y}$ plane. Regions marked I, II, and III respectively represent multiscaling, simple scaling different from the linear theory, and the effectively linear model.

$d < 2$ follows; for $y < d$, model I becomes effectively linear in the long-wavelength limit and shows $z = 2$ and $\chi = (2 - d + \overline{y})/2$. These considerations are used to obtain a phase diagram in the y-$\overline{y}$ plane showing phase space regions with multiscaling and simple scaling; see Fig. 3.

VI. MULTISCALING IN MODEL II

We consider now how the multiscaling properties in model I elucidated above gets modified when **v** satisfies Eq. (12). Here, the velocity is *not* temporally δ-correlated (unlike model I); instead the relaxation time of the velocity modes are q-dependent. A notable quantitative difference is that in model II ($\Gamma = \eta q^2$), $D^v_{ij}(q,\omega = 0)$ is more divergent than in model I for the same y. To calculate the multiscaling exponents, we follow the same logic as outlined in Sec. V.

We first find corrections to the relevant model parameters by using the action functional (26). The relevant Feynman diagrams are identical to those in model I and are given in Figs. 6 and 7, which are to be evaluated for $\Gamma = \eta q^2$. As above, we first consider $\overline{y} = -2$. We find the following one-loop corrections:

$$\nu^< = \nu + \frac{K_d(d-1)D_1\lambda^2\Lambda^{d-y-2}}{\nu d(d-y-2)}[1 - b^{y+2-d}],$$
$$D_0^< = D_0 + \frac{K_d(d-1)D_1D_0\lambda^2\Lambda^{d-y-2}}{\nu^2 d(d-y-2)}[1 - b^{y+2-d}]. \quad (64)$$

As in model I, there are no relevant corrections to λ at the one-loop order. Upon using the same rescaling procedure employed for model I (see Appendix B for details), we arrive at the following flow equations:

$$\frac{d\nu}{dl} = \nu[z - 2 + \overline{g}], \quad (65)$$

$$\frac{dD_0}{dl} = D_0[z - 2\chi - d - 2 + \overline{g}], \quad (66)$$

and

$$\frac{d\lambda}{dl} = \lambda\left[\frac{y + z - d}{2} - 1\right], \quad (67)$$

where $\overline{g} = \frac{K_d(d-1)D_1\lambda^2\Lambda^{d-y-2}}{\nu^2 d(d-y-2)}$ is an effective coupling constant. The flow equation for $\overline{g}$ takes the form

$$\frac{d\overline{g}}{dl} = \overline{g}[y - d + 2 - 2\overline{g}]. \quad (68)$$

Thus, the FP values for $\overline{g}$ evaluate to $\overline{g}^* = 0$ and $\overline{g}^* = (y - d + 2)/2$. Clearly, $\overline{g}^* = 0$ is the stable FP for $y \leqslant d - 2$ while for $y > d - 2$, $\overline{g}^* = (y - d + 2)/2$ is the stable FP. We look for multiscaling with $0 < \overline{g}^* \ll 1$, i.e., $0 < y - d + 2 \ll 2$.

As in model I, here we have $z = 2$ for $y \leqslant d - 2$ and for $y > d - 2$,

$$z = \frac{2 - y + d}{2} < 2, \quad (69)$$

since $\overline{g}^* > 0$. Interestingly, the spatial scaling exponent $\chi = \frac{-d}{2}$ for both the FP values of $\overline{g}$, a value unchanged from model I (with $\overline{y} = -2$ there). Thus χ remains unchanged in model II when $\overline{y} = -2$. As argued for model I, this rules out multiscaling in model II for $\overline{y} = -2$. Following the logic outlined in Sec. V, we find

$$\zeta_{2n} = 2n\chi = -nd, \quad \zeta_2 = -d, \quad (70)$$

identical to model I (with $\overline{y} = -2$).

Next, consider $\overline{y} > -2$, again similar to the corresponding study on model I. We then find for $y > d - 2$

$$\chi = (z - d - 2 + \overline{y})/2 = \left[\frac{2 - y + d}{2} - d - 2 + \overline{y}\right]\Big/2. \quad (71)$$

Equation (71) again shows that χ can turn positive depending on the interplay between $\overline{y}$ and y and thus may lead to multiscaling. Dynamic exponent z is still given by $z = \frac{2-y+d}{2} < 2$, independent of $\overline{y}$. Below we investigate the possibility of multiscaling when $\chi > 0$.

We now carry out exactly the same analysis for the composite operators $\mathcal{O}_n(\mathbf{x})$ as for model I, and obtain their one-loop renormalized scaling dimension Δ_{2n}. Expectedly, $\overline{g}^* = (y - d + 2)/2 = \delta_2$ plays the role of ϵ in Ref. [9]. We find

$$\Delta_{2n} = 2n(\chi - 1) + \frac{\overline{g}^* n(d + 2n)}{d + 2}$$
$$= n(z - d + \overline{y} - 2) + \frac{n(y + 2 - d)(d + 2n)}{2(d + 2)}. \quad (72)$$

Assuming positive Δ_{2n}, as necessary for multiscaling, we obtain for ζ_{2n}

$$\zeta_{2n} = 2n - \frac{\overline{g}n(d + 2n)}{(d + 2)}. \quad (73)$$

For $\overline{g}^* = (y + 2 - d)/2 = \delta_2$, we have

$$\zeta_{2n} = 2n - \frac{n(y + 2 - d)(d + 2n)}{2(d + 2)}, \quad (74)$$

$$\zeta_2 = 2 - \frac{y + 2 - d}{2} = 2 - \delta_2, \quad (75)$$

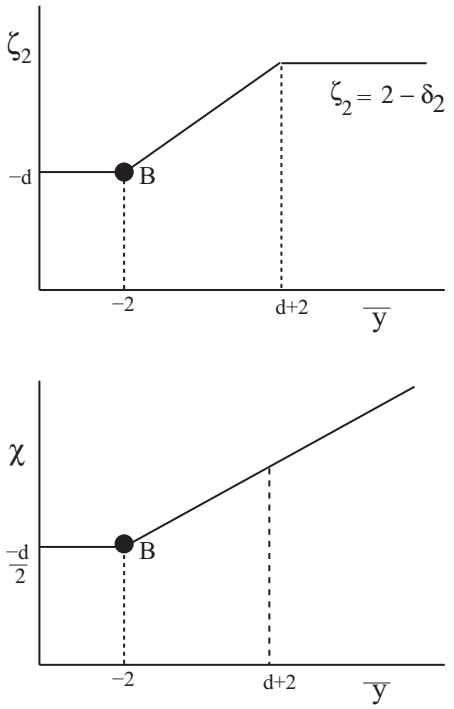

FIG. 4. Schematic plot of ζ_2 (top) and χ (bottom) versus $\overline{y}$ for model II (for $\delta_2 > 0$). Similarly to model I, here too ζ_2 and χ vary linearly with $\overline{y}$ for $-2 < \overline{y} < d+2$ and have a *finite* discontinuity (marked by B) at $\overline{y} = -2$. This is in contrast to model I (see text). In the multiscaling regime, i.e., for $\overline{y} > d+2$, ζ_2 again saturates, while χ keeps growing linearly; see text.

which have no explicit dependence on $\overline{y}$, similarly to (59) for model I; see also Ref. [33] for related discussions. As in model I, for a fixed δ_2, ζ_2 does not depend on d explicitly, but all of $\zeta_{2n}, n > 1$, do. At $d = 3$, $\zeta_2 = 2 - \delta_2$, $\zeta_{2n} = 2n - n\delta_2(3 + 2n)/5, n > 1$. This is similar to model I, and is parametrized by $\delta_2 > 0$ which remains undetermined. Again similar to model I, the threshold on $\overline{y}$ for multiscaling can be obtained from Δ_{2n}. Demanding that all of Δ_{2n} must not be negative for multiscaling (see the analogous discussions for model I in Sec. V above), we note that Δ_2 vanishes for $\overline{y} = d+2$, with all other $\Delta_{2n} > 0$ for $n > 1$ even when $\overline{g}^* \ll 1$. Thus $\overline{y} = d+2$ sets the threshold for multiscaling with vanishingly small $\overline{g}^* \ll 1$ as required for the validity of our one-loop perturbation theory; this is the analog of the threshold $\overline{y} = d$ for multiscaling in model I. Hence, model II multiscales for $\overline{y} \geqslant d+2$, $y > d-2$, where as for $\overline{y} < d+2$, multiscaling vanishes. For $\overline{y} < d+2$ and $y > d-2$, model II shows simple scaling with z and χ given by (69) and (71), respectively, along with

$$\zeta_{2n} = 2n\chi = n\left[\frac{2-y+d}{2} - d - 2 + \overline{y}\right], \tag{76}$$

$$\zeta_2 = 2\chi = \frac{2-y+d}{2} - d - 2 + \overline{y} = \overline{y} - d - \delta_2. \tag{77}$$

Thus ζ_2 as a function of $\overline{y}$ does *not* vary continuously, as is evident from (70), (75), and (77). How χ and ζ_2 depend on $\overline{y}$ in model II is shown schematically in Fig. 4.

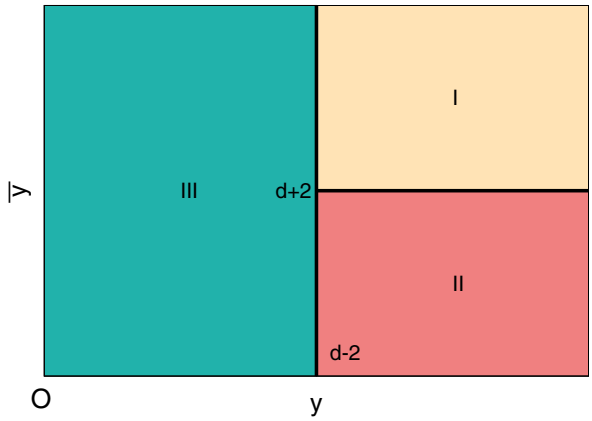

FIG. 5. Phase diagram of model II in the y-$\overline{y}$ plane. Regions marked I, II, and III respectively represent multiscaling, simple scaling different from the linear theory, and the effectively linear model. The general structure of the phase diagram is the same as the phase diagram for model I; see Fig. 3.

Notice that at the threshold $\overline{y} = d+2$, we have $\chi = z/2 = (2-y+d)/4 = 1 - \frac{\overline{g}}{4}$ that approaches unity for $\overline{g} \ll 1$. Lastly for all $\overline{y}$ but $y < d-2$, model II becomes effectively linear in the hydrodynamic limit and simple scaling with z and χ as given by (30) hold. Similarly to model I, the behavior for $\overline{y} < -2$ is identical to $\overline{y} = -2$. As for model I, these considerations may be used to obtain a phase diagram in the y-$\overline{y}$ plane; see Fig. 5.

VII. SUMMARY

We have thus elucidated how the multiscaling exponents of the equal-time structure functions $\mathcal{S}_{2n}(r)$ for the concentration θ of a substance in a self-similar turbulent flow may be extracted. By using two different models, model I and model II, we establish that both the advective velocity as well as the additive noise must have variances that are spatially long range for $\mathcal{S}_{2n}(r)$ to display multiscaling. We show that while $\overline{y}$ that characterizes the spatial scaling of the additive noise variance must exceed its threshold ($=d, d+2$) for multiscaling to be observed, the multiscaling exponents ζ_{2n} do not explicitly depend on them. Rather the L dependencies of the structure functions $\mathcal{S}_{2n}$ become stronger with increase in $\overline{y}$, a feature shared by both model I and model II. These results complement the existing studies. In addition, these should be of significance for studies of scaling in dynamical models driven by long-range noises.

Model I and model II differ principally by the choice of the associated correlation of the advecting velocity $\mathbf{v}$: for model I $\mathbf{v}$ is δ-correlated in time, whereas for model II, it has a q-dependent correlation time that is finite for finite q. Despite this significant difference, both model I and model II are shown to display multiscalings for $\mathcal{S}_{2n}(r)$ that are qualitatively similar to each other. This shows the robustness of the physical mechanism responsible for multiscaling as elucidated here. For both models, the additive noise in the concentration equation must be long-ranged for multiscaling to occur: we show $\overline{y} = d$ and $\overline{y} = d+2$ are the multiscaling thresholds, respectively, for model I and model II. At the same time, $y > d$ (for model I)

and $y > d - 2$ (for model II) are also necessary conditions for multiscaling. For values of $\overline{y}$ and y outside the ranges necessary for multiscaling, the system shows simple scaling. We use our scheme of calculations to explore the whole $\overline{y}$-y plane and identify phase space regions corresponding to scaling or multiscaling. Our studies may be straightforwardly applied to the problem of *passive vector turbulence* [35], where a vector field, instead of a scalar concentration, is advected by a turbulent velocity and displays multiscaling akin to the multiscaling elucidated here. We note here that the control parameters used in our models and those used in [23,24] are different. While the q dependence of the ratio of different timescales was a control parameter in [23,24], in our models the control parameters are y and $\overline{y}$.

The quantitative accuracy of our results is limited by the low order of the perturbation theory used. It may be noticed that for very high n or y, ζ_{2n} can become negative, a feature not observed in experiments. In fact, the results from both model I and model II for sufficiently small δ_1 or δ_2 appear close enough with the results on the exponent ratio ζ_{2n}/ζ_2 for low orders (i.e., low n) as reported in Ref. [16]; for high enough orders there are significant departures between the perturbative results here and those in Ref. [16]. Indeed, direct quantitative comparisons of the perturbatively obtained values of ζ_{2n} in model I or model II with experimental results are difficult due to the explicit appearances of $\delta_1 > 0$ or $\delta_2 > 0$ as free parameters in the expressions for ζ_{2n} in model I and model II respectively, which cannot be pinned down to specific numerical values in our scheme of calculations. One possible way to fix them would be to compare any one of the ζ_{2n} with the corresponding experimentally obtained value and then use the value of δ_1 or δ_2 so obtained to calculate the remaining ζ_{2n}. Nevertheless, this remains somewhat *ad hoc* and we do not pursue this here. For better convergence of the perturbative results, higher-order fluctuation corrections are to be included for higher values of n or y. Both model I and model II are idealized limits of the more challenging real problem, *viz.*, the active scalar hydrodynamics. In this problem, the feedback of the concentration θ on the advecting fluid is kept and the velocity satisfies the generalized Navier-Stokes equation [36,37]. Structure functions for both $\mathbf{v}$ and θ are expected to display nontrivial multiscaling [37], similarly to forced magnetohydrodynamic (MHD) turbulence, where both velocity and magnetic fields are known to display multiscaling [38]. A systematic and controlled perturbative approach to multiscaling in these systems still remains elusive, a major obstacle being the nonlinear form of the underlying equations of motion in both $\mathbf{v}$ and θ (or in velocity and magnetic fields for MHD turbulence). Despite the simplicity of model I and model II used here, we hope our work will be a step forward in the right direction towards solving the full nonlinear problems. In this work, we have studied *static* multiscaling, i.e., the multiscaling of equal-time structure functions. These have been generalized to *dynamic multiscaling* of time-dependent structure functions [39]. It has been shown both numerically and analytically that the Kraichnan passive scalar model *does not* show any dynamic multiscaling [40]. Whether this remains true for all $\overline{y} \geqslant d$ for model I and all $\overline{y} > d + 2$ for model II are not known. How our framework of calculations used above may be extended to study these questions and dynamic multiscaling of a passively advected concentration in general remains a challenging task for the future. Lastly, our studies here should be important in building the general understanding of universal scaling in driven, diffusive models with long-range noises, e.g., in the context of the studies reported in Ref. [41].

ACKNOWLEDGMENT

The authors thank the Alexander von Humboldt Stiftung, Germany, for partial financial support through the Research Group Linkage Programme (2016).

APPENDIX A: BARE PROPAGATORS AND CORRELATORS

We identify the propagators and correlators of the system:

$$\begin{aligned}
\langle\hat{\theta}(\mathbf{q},\omega)\hat{\theta}(-\mathbf{q},-\omega)\rangle &= 0,\\
\langle\hat{\theta}(\mathbf{q},\omega)\theta(-\mathbf{q},-\omega)\rangle &= \frac{-1}{-i\omega+\nu q^2},\\
\langle\hat{\theta}(-\mathbf{q},-\omega)\theta(\mathbf{q},\omega)\rangle &= \frac{-1}{i\omega+\nu q^2},\\
\langle\theta(\mathbf{q},\omega)\theta(-\mathbf{q},-\omega)\rangle &= \frac{2D_0q^2}{\omega^2+\nu^2q^4}.
\end{aligned} \tag{A1}$$

APPENDIX B: ONE-LOOP CORRECTIONS TO ν AND D_0 IN MODEL I FOR $\overline{y} = -2$

The one-loop corrections to ν (Fig. 6) and D_0 (Fig. 7) respectively are

$$\delta\nu = \frac{K_d(d-1)A\lambda^2\Lambda^{d-y}}{d(d-y)}[1-b^{y-d}] \tag{B1}$$

and

$$\delta D_0 = \frac{K_d(d-1)D_0A\lambda^2\Lambda^{d-y}}{d(d-y)}[1-b^{y-d}]. \tag{B2}$$

The corrected model parameters (marked by subscript "<") thus take the following forms:

$$\nu^< = \nu + \delta\nu, \quad D_0^< = D_0 + \delta D_0, \quad \lambda^< = \lambda. \tag{B3}$$

The rescaled model parameters can then be written in terms of the scale factor b:

$$\begin{aligned}
\nu' &= b^{z-2}\nu^<,\\
D_0' &= \xi_R^{-2}b^{z-d-2}D_0^<,\\
\lambda' &= \xi_{vR}b^{z-1}\lambda.
\end{aligned} \tag{B4}$$

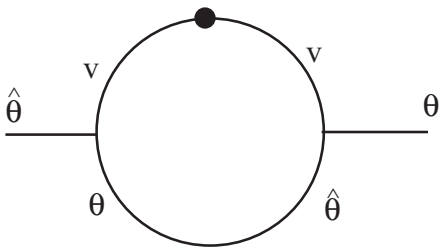

FIG. 6. One-loop diagram for ν.

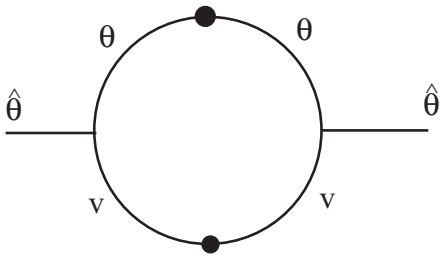

FIG. 7. One-loop diagram for D_0.

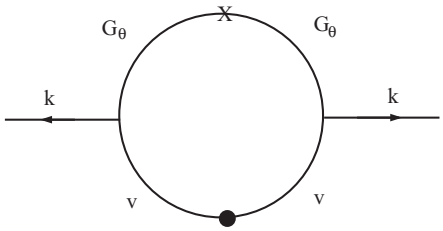

FIG. 8. One-loop diagram that corrects $\mathcal{O}_n$. The X refers to $\mathcal{O}_n$; $G_\theta = \langle\hat{\theta}(-\mathbf{q},-\omega)\theta(\mathbf{q},\Omega)\rangle$.

APPENDIX C: COMPOSITE OPERATORS

Here we calculate the one-loop correction to the composite operators $\mathcal{O}_n(\mathbf{x}) = [\partial_i\theta(\mathbf{x})]^{2n}$. The relevant one-loop diagram is shown in Fig. 8. The one-loop diagram in Fig. 8 may be constructed by contracting two of the θ fields in $\mathcal{O}_n(\mathbf{x})$ with two trilinear nonlinearities, each of the form $\lambda\hat{\theta}\mathbf{v}\cdot\boldsymbol{\nabla}\theta$ (we have suppressed the space-time indices for notational convenience). The resulting diverging one-loop integral is as given in (50).

[1] G. Falkovich *et al.*, Rev. Mod. Phys. **73**, 913 (2001).
[2] U. Frisch, *Turbulence: The Legacy of A. N. Kolmogorov* (Cambridge University Press, Cambridge, 1995).
[3] A. N. Kolmogorov, C. R. Acad. Sci. URSS **30**, 301 (1941).
[4] For reviews see K. R. Sreenivasan and R. A. Antonia, Annu. Rev. Fluid Mech. **29**, 435 (1997); S. K. Dhar, A. Sain, A. Pande, and R. Pandit, Pramana **48**, 325 (1997).
[5] E. Brézin, J. C. L. Guillon, and J. Zinn-Justin, *Phase Transitions and Critical Phenomena* (Academic Press, New York, 1976), Vol. 6; J. Zinn-Justin, *Quantum Field Theory and Critical Phenomena* (Clarendon Press, Oxford, 2010).
[6] L. M. Smith and S. W. Woodruff, Annu. Rev. Fluid Mech. **30**, 275 (1998).
[7] A. M. Obukhov, Izv. Akad. Nauk SSSR, Ser. Geogr. Geofiz. **13**, 58 (1949).
[8] R. H. Kraichnan, Phys. Rev. Lett. **72**, 1016 (1994).
[9] L. Ts. Adzhemyan, N. V. Antonov, and A. N. Vasil'ev, Phys. Rev. E **58**, 1823 (1998).
[10] K. Gawedzki and A. Kupiainen, Phys. Rev. Lett. **75**, 3834 (1995).
[11] C. Pagani, Phys. Rev. E **92**, 033016 (2015).
[12] M. Chertkov, G. Falkovich, I. Kolokolov, and V. Lebedev, Phys. Rev. E **52**, 4924 (1995); M. Chertkov and G. Falkovich, Phys. Rev. Lett. **76**, 2706 (1996); D. Bernard, K. Gawędzki, and A. Kupiainen, Phys. Rev. E **54**, 2564 (1996).
[13] M. Holzer and E. D. Siggia, Phys. Fluids **6**, 1820 (1994).
[14] S. Chen and R. H. Kraichnan, Phys. Fluids **10**, 2867 (1998).
[15] I. Mazzitelli and A. S. Lanotte, Physica D **241**, 251 (2012).
[16] F. Moisy, H. Willaime, J. S. Andersen, and P. Tabeling, Phys. Rev. Lett. **86**, 4827 (2001).
[17] G. Ruiz-Chavarria, C. Baudet, and S. Ciliberto, Physica D **99**, 369 (1996).
[18] L. Ts. Adzhemyan and N. V. Antonov, Phys. Rev. E **58**, 7381 (1998); N. V. Antonov, Physica D **144**, 370 (2000); N. V. Antonov, N. M. Gulitskiy, M. M. Kostenko, and T. Lucivjanský, Phys. Rev. E **95**, 033120 (2017).
[19] M. Gauding, L. Danaila, and E. Varea, Int. J. Heat Fluid Flow **67**, 86 (2017).
[20] R. A. Antonia, E. J. Hopfinger, Y. Gagne, and F. Anselmet, Phys. Rev. A **30**, 2704 (1984).
[21] N. V. Antonov and A. V. Malyshev, J. Stat. Phys. **146**, 33 (2012).
[22] B. Schmittmann, Int. J. Mod. Phys. B **04**, 2269 (1990).
[23] N. V. Antonov, Phys. Rev. E **60**, 6691 (1999).
[24] L. Ts. Adzhemyan, N. V. Antonov, and J. Honkonen, Phys. Rev. E **66**, 036313 (2002).
[25] C. De Dominicis, J. Phys. Colloques **37**, C1-247 (1976).
[26] P. M. Chaikin and T. C. Lubensky, *Principles of Condensed Matter Physics* (Cambridge University Press, Cambridge, 2000).
[27] P. C. Hohenberg and B. I. Halperin, Rev. Mod. Phys. **49**, 435 (1977).
[28] D. Forster, D. R. Nelson, and M. J. Stephen, Phys. Rev. A **16**, 732 (1977).
[29] U. Täuber, *Critical Dynamics* (Cambridge University Press, Cambridge, 2014).
[30] J. Cardy, G. Falkovich, and K. Gawedzki, *Non-equilibrium Statistical Mechanics and Turbulence* (Cambridge University Press, Cambridge, 2008).
[31] A. N. Vasil'ev, *The Field Theoretic Renormalization Group in Critical Behavior Theory and Stochastic Dynamics* (Chapman and Hall/CRC Press, Boca Raton, 2004).
[32] One may also consider composite operators of the form $(\partial_t\theta\partial_t\theta)^m$, or suitable products of $\partial_t\theta$ and $\boldsymbol{\nabla}\theta$ that are scalar. However in the hydrodynamic limit, invoking dynamical scaling we note that any operator involving one or more $\partial_t\theta$ will be subleading to the operator having the same number of θ, but only with $\boldsymbol{\nabla}$ acting on θ, so long as the dynamic exponent $z > 1$. We show below that $z > 1$ within the low-order perturbation theory used here, and thus neglect composite operators involving $\partial_t\theta$.
[33] L. Ts. Adzhemyan *et al.*, *The Field Theoretic Renormalization Group in Fully Developed Turbulence* (Gordon and Breach, Amsterdam, 1999).
[34] It is conceivable that $\Delta_{2n} < 0$ for $n \leqslant m$ some integer $m > 1$, and $\Delta_{2n} > 0$ for $n > m$, apparently implying "multiscaling" for higher-order structure functions, but simple scaling for the lower-order ones. For a "small" $y - d = \delta_1 \ll 1$, necessary for the validity of our low-order perturbation calculations, such a possibility is ruled out and we exclude these from our considerations here.

[35] N. V. Antonov and N. M. Gulitskiy, Lect. Notes Comput. Sci. **7125**, 128 (2012).
[36] R. Ruiz and D. R. Nelson, Phys. Rev. A **23**, 3224 (1981).
[37] S. S. Ray and A. Basu, Phys. Rev. E **84**, 036316 (2011).
[38] A. Basu, A. Sain, S. K. Dhar, and R. Pandit, Phys. Rev. Lett. **81**, 2687 (1998).
[39] D. Mitra and R. Pandit, Phys. Rev. Lett. **93**, 024501 (2004); S. S. Ray, D. Mitra, and R. Pandit, New J. Phys. **10**, 033003 (2008).
[40] D. Mitra and R. Pandit, Phys. Rev. Lett. **95**, 144501 (2005).
[41] E. Medina, T. Hwa, M. Kardar, and Y.-C. Zhang, Phys. Rev. A **39**, 3053 (1989).